Environmental Science
Water Research & Technology

PAPER

View Article Online
View Journal | View Issue

Cite this: *Environ. Sci.: Water Res. Technol.*, 2016, **2**, 1004

Trihalomethane, dihaloacetonitrile, and total *N*-nitrosamine precursor adsorption by carbon nanotubes: the importance of surface oxides and pore volume†

Erin M. Needham,[a] Shelby M. Sidney,[a] Justin R. Chimka[b] and Julian L. Fairey*[a]

Received 28th July 2016,
Accepted 27th September 2016

DOI: 10.1039/c6ew00193a

rsc.li/es-water

As drinking water sources become increasingly impaired, enhanced removal of natural organic matter (NOM) may be required to curb formation of disinfection byproducts (DBPs) upon chlor(am)ination. While carbon nanotubes (CNTs) can adsorb NOM, their properties for DBP precursor adsorption have not been elucidated. Nine types of CNTs were assessed for trihalomethane (THM), dihaloacetonitrile (DHAN), and total *N*-nitrosamine (TONO) precursor adsorption. Batch isotherm experiments were completed with lake water and, to simulate an impaired condition, effluent from a wastewater treatment plant (WWTP). Adsorption varied with CNT type and dose, with TONO precursors having the highest percent removals from WWTP effluent (up to 97%). Physicochemical properties of CNTs were characterized by gas adsorption isotherms and X-ray photoelectron spectroscopy and numerical models were developed to identify CNT properties driving DBP precursor adsorption. The models fits were strong ($R^2 > 0.92$) and indicated removal of the three precursor types increased with percent carboxyl groups ($p < 0.01$) and, for TONO precursors only, cumulative pore volume (CPV, $p = 0.001$). A multicollinearity analysis suggested surface oxides – particularly carboxyl groups – on the CNTs increased CPV, presumably by increasing electrostatic repulsive forces, which enhanced microporosity sufficiently to overshadow any repulsion of DBP precursors from negatively charged surface oxides. A size exclusion analysis revealed all CNT pores were accessible to TONO precursors, while THM and DHAN precursors had limited access to the smaller micropores. These findings provide a framework to modify CNTs to optimize adsorption of DBP precursors and demonstrate the potential of CNTs for TONO precursor removal.

Water impact

Carbon nanotubes were evaluated for their efficacy to adsorb precursors of trihalomethanes, dihaloacetonitriles, and *N*-nitrosamines. The results provide a framework to modify CNTs for enhanced adsorption of these disinfection byproduct precursors.

1. Introduction

The tunable physicochemical properties of carbon nanotubes (CNTs)[1,2] have the potential to be exploited in drinking water treatment plants (DWTPs) to adsorb organic precursors of disinfection byproducts (DBPs). While CNT toxicity[3,4] is a concern in water treatment, the technology is now available to grow CNTs on various substrates as well as to incorporate CNTs into membrane filtration systems.[1] This may alleviate problems associated with fate and transport of toxic substances related to CNTs[5] in drinking waters. However, before CNT-based attached growth or membrane applications can be developed specifically to enhance DBP precursor removal, fundamental investigations are needed to quantify the affinity of CNTs for important groups of DBP precursors and elucidate the physiochemical properties primarily responsible for their adsorption.

It is well known that natural organic matter (NOM) in source water reacts with disinfectants (*i.e.*, free chlorine or chloramines) to form DBPs at low μg L^{-1} levels, such as trihalomethanes (THMs)[6] and dihaloacetonitriles (DHANs).[7] In waters enriched with algal organic matter or impacted by wastewater treatment plant (WWTP) effluents, *N*-nitrosamines

[a] *Department of Civil Engineering, University of Arkansas, Fayetteville, AR 72701, USA. E-mail: julianf@uark.edu; Fax: +(479) 575 7168; Tel: +(479) 575 4023*
[b] *Department of Industrial Engineering, University of Arkansas, Fayetteville, AR 72701, USA*

† Electronic supplementary information (ESI) available. See DOI: 10.1039/c6ew00193a

can also form, albeit at low ng L^{-1} levels.[8] *N*-nitrosamines are a non-halogenated group of DBPs under consideration for regulation in drinking waters due to their high toxicity.[9] While the majority of *N*-nitrosamine research to date has focused on *N*-nitrosodimethylamine (NDMA) due to its prevalence in drinking water systems,[10] recent studies have demonstrated NDMA may only comprise ~5% of total *N*-nitrosamines (TONO) in chloramine systems.[11] As such, relatively little is known about the removal of TONO precursors by engineered sorbents, although a recent study demonstrated that they have some affinity for activated carbon.[12] Further, the authors are aware of no studies that have assessed the concomitant removal of THM, DHAN, and TONO precursors in sorption processes. With respect to CNTs, other researchers have demonstrated their affinity for various NOM fractions in water,[5,13] although these investigations were geared towards minimizing NOM uptake by CNTs to maximize adsorption of other target compounds. Regardless, development of novel sorbents with enhanced affinities for organic DBP precursors could potentially be leveraged to curb DBP formation in finished drinking waters, regardless of the disinfection scheme used.

As DBP measurements are time- and labor-intensive, reliable DBP precursor surrogate measures can be valuable screening tools to assess treatment. Previous studies by this research group have demonstrated metrics from fluorescence excitation–emission matrices (EEMs) collected before and after treatment but prior to chlor(am)ination were strong total THM (TTHM) precursor surrogates.[14] In these studies, the EEMs were decomposed by parallel factor analysis (PARAFAC) to identify principal fluorophore groups.[15] The corresponding maximum intensity values, F_{MAX}, of humic- and fulvic-like fluorophores correlated strongly with TTHM precursor concentrations. A more recent study found strong correlations between fluorescence intensity values from peak-picking (*i.e.*, excitation–emission pairs, $I_{Ex/Em}$) and removal of TTHM and DHAN precursors.[16] There is, however, a strong basis for why fluorescence may be useful as a TONO precursor surrogate. For example, in contrast to EPA method 521 *N*-nitrosamines, algal-derived organic matter is a strong precursor to uncharacterized *N*-nitrosamines measured by the TONO assay.[8] Additionally, Liao and colleagues found strong correlations between the removal of NA9FP – the sum of the FP of the six *N*-nitrosamines regulated under the UCMR2 along with *N*-nitrosomorpholine, *N*-nitrosopiperidine, and *N*-nitrosodiphenylamine – and the regions of a fluorescence EEM associated with aromatic proteins (R = 0.88) and soluble microbial products (R = 0.90).[17] Aromatic proteins are nitrogen-containing and *N*-nitrosamine precursors can be present as functional groups, while soluble microbial products have been identified as an NDMA precursor.[8] In essence, secondary, tertiary, and quaternary amines may not fluoresce themselves but may be associated with compounds that do so. Coupled with the labor-intensive nature of TONOFP tests, a fluorescence-based TONO precursor surrogate would advance development of control measures for these DBPs.

Given that the structure of CNTs is equivalent to that of a rolled graphene sheet, their physicochemical properties dictate their functionality. CNTs can be produced in single-walled (SW) and multi-walled (MW) varieties, both of which have high specific surface area and range in hydrophobicity,[5,13] size,[18] shape,[1] texture,[19] defects,[20] and functionalities,[21] all of which can be manipulated for their intended application. The ability to fine-tune CNT properties is an attractive option for use as a sorbent in drinking water treatment, but it is not yet known what properties are desirable for DBP precursor removal. Adsorption by CNTs is based on accessible surface area, which includes aggregated pores and large external surface area, in contrast to activated carbon, which preferentially adsorbs lower molecular weight compounds due to size exclusion from micropores. CNTs have been shown to have high adsorption capacities for organic contaminants[22] and to outperform other microporous adsorbents in competitive adsorption systems.[23]

The objective of this study is to assess physicochemical CNT properties for enhanced TTHM-, DHAN-, and TONO-precursor adsorption. Nine commercially available CNTs were selected with a variety of characteristics and used in batch isotherm tests with two diverse water sources – a well-characterized lake water[24] that serves as a drinking water source and an effluent from a conventional WWTP. The TTHM-, DHAN-, and TONO-precursor concentrations in the raw and CNT-treated waters were indirectly measured using a recently verified DBP formation potential (DBPFP) test,[16] modified from Standard Methods 5710-B and D.[25] Each CNT type was characterized physically by gas adsorption isotherms to determine their specific surface area and pore volume distributions, and chemically by X-ray photoelectron spectroscopy (XPS) to determine the relative composition of surface functional groups. These physicochemical properties were used as primary variables in models to assess the adsorption of TTHM-, DHAN-, and TONO-precursors. Modeling results revealed strong correlations between CNT properties and removal of all three DBP precursor types. The findings of this study provide guidance for selective modification of CNTs for enhanced DBP precursor adsorption.

2. Materials and methods

2.1. Site description and sample collection

Waters used for the isotherm experiments originated from Beaver Lake, the drinking water source for Northwest Arkansas, and the West Side Wastewater Treatment Plant (WS-EFF) in Fayetteville, AR. Beaver Lake water (BL-RAW) was collected at the intake structure of the Beaver Water District DWTP (Lowell, AR) on July 7, 2014. Details on the land use and nutrient inputs in the Beaver Lake watershed can be found elsewhere.[24] WS-EFF samples were collected June 6, 2014 from the WWTP effluent. The plant utilizes biological nutrient removal, depth filtration, and ultraviolet disinfection with effluent aeration prior to discharge. Raw water characteristics are detailed in Table S1.† Both waters were stored in 50 L

low-density polyethylene carboys at 4 °C in the dark prior to use in the isotherm experiments.

2.2. Experimental procedures

2.2.1. Bottle-point isotherms. Bottle-point isotherms were conducted with nine types of commercially available CNTs, selected to cover a range of wall type (SW and MW), diameter, and length (Table S2†). CNTs were added to the sample waters at doses of 0, 25 and 50 mg L^{-1}, in triplicate, in 1.25 L headspace-free amber glass bottles and were tumbled end-over-end for 3 days. Lu *et al.*[26] showed that 4 hours was sufficient to reach equilibrium in a bottle-point isotherm study with MWCNTs and NOM-spiked waters. An equilibrium time of 3 days (*i.e.*, 18 times longer) was chosen in this study and assumed to be a sufficient equilibration period for all precursors given the diversity of DBP precursors in the sample waters, including those for TONO for which little characterization information exists. The pH drift during the 3 days of tumbling was less than 0.1 pH unit from the initial values reported in Table S1.† CNT doses were chosen to achieve less than 100% removal based on preliminary TTHMFP and DHANFP removal tests, the results of which are detailed in Table S3.† It is important to note that the goal of this study does not include determination of the required CNT doses at a DWTP; rather, this study is intended identify CNT properties for enhanced DBP precursor adsorption and future studies will focus on development of an optimized CNT type and application mode. Following tumbling, BL-RAW samples were filtered through pre-rinsed 0.45 μm polyethersulfone (PES) membranes.[27] The WS-EFF samples were passed through pre-rinsed 0.7 μm glass fiber filters prior to 0.45 μm PES filtration, as direct filtration with the PES membranes was impractically slow. In both cases, filtration removed all CNTs from the water samples, which was confirmed by the lower chlorine residuals (or higher demand) of the blank relative to the CNT-treated waters (Table S4†). Methods used for measuring dissolved organic carbon (DOC) and fluorescence EEMs, and performing PARAFAC analysis are in the ESI.†

2.2.2. DBPFP. The procedure developed by Do *et al.*[16] was used to assess the DBPFP of untreated waters (*i.e.*, samples not exposed to CNTs) and CNT-treated waters and is detailed in the ESI.† EPA method 551.1 with modifications[28] was used to extract TTHMs and DHANs into *n*-pentane. A gas chromatograph equipped with an electron capture detector (GC-ECD, Shimadzu 2010) was used to quantify TTHMFP (the sum of trichloromethane, dichlorobromomethane, dibromochloromethane, and tribromomethane formation potential) and DHANFP (the sum of dichloroacetonitrile, bromochloroacetonitrile, and dibromoacetonitrile formation potential). Details regarding the GC standard curve are provided in the ESI.† Blanks and check standards complied with EPA method 551.1.

Assessment of total *N*-nitrosamine formation potential (TONOFP) began with a modified SPE procedure from EPA method 521, adapted from Kulshrestha *et al.*[29] SPE columns were conditioned with methanol and Milli-Q water, and then 500 mL sample aliquots were pulled through the columns at a flow rate of 5 mL min^{-1}. Following 10 minutes of column aspiration, *N*-nitrosamines were eluted from the SPE columns using 12 mL of methanol. All remaining water was removed from the column extracts using a sodium sulfate drying column rinsed with an additional 3 mL of methanol; leached sodium sulfate was subsequently removed with a 0.2 μm nominal pore size polytetrafluoroethylene syringe filter. Samples were concentrated to 1 mL in a 37 °C water bath using an evaporator with ultra high purity nitrogen gas and stored at −20 °C. To eliminate potential interferences, *S*-nitrosothiols and nitrite, if present, were quenched immediately before TONO measurement from sample extracts with 20 g L^{-1} mercuric chloride in Milli-Q water and 50 g L^{-1} sulfanilamide in 1 N HCl, respectively. Notably, ion chromatography results (Table S1†) indicated no nitrite in raw waters (method detection limit, MDL = 0.008 mg L^{-1}). An Eco Physics CLD 88sp chemiluminescence NO detector was used to quantify *N*-nitrosamines in purified samples, as detailed in Mitch and Dai.[30] TONO concentrations were determined using a five-point NDMA standard curve, which was rerun after every four samples to account for sample mass recoveries. To prevent sample carryover, blank spike samples were run between each sample. As untreated BL-RAW samples had average TONO concentrations of 33 ng L^{-1} as NDMA, just above the MDL of this procedure, TONO was not measured for these CNT-treated samples.

2.2.3. CNT characterization. CNT physical characteristics were measured rather than relying on manufacturer specifications (Table S2†). The pore volume distribution and Brunauer–Emmett–Teller (BET) surface area of the CNTs were measured using a Quantachrome Nova 2200e surface area and pore size analyzer using N_2 and CO_2 gas adsorption at 77 K and 273 K, respectively. Adsorption isotherms (Fig. S1†) were collected at partial pressures of 0.005–0.99 using step sizes of 0.011–0.095. Pore volume distributions (Fig. S2†) were calculated from the isotherms using a hybrid density functional theory model that assumed slit pore geometry for micropores and slit or cylindrical pore geometry for mesopores.[31] The BET surface area (S_{BET}) was calculated using the N_2 adsorption isotherm in the linear relative pressure range from 0.05–0.30. However, it should be noted that S_{BET} is calculated without regard for the information given about micropores by the CO_2 adsorption isotherm. As such, S_{BET} is more suitable for comparing the amount of specific surface area individual CNT types have relative to each other, rather than their absolute specific surface area.[31]

XPS measurements were performed on pristine CNTs using a PHI 5000 VersaProbe spectrometer with an AlKα source, and a vacuum of 10^{-8} Torr was maintained during analysis. Methods for the XPS data analysis are detailed in the ESI† and carbon spectra deconvolutions are shown in Fig. S3.†

2.2.4. Data modeling. To assess the impact of physicochemical CNT characteristics on DBP precursor adsorption, a

multivariate analysis was performed for the three groups of DBPs. DBPFP was expressed as a ratio, as the median of each triplicate sample to the median of each untreated sample – either BL-RAW or WS-EFF, as appropriate. The median was utilized, rather than the mean, due to its relative insensitivity to outliers. The potential undue influence on the mean caused by outliers in the data is exacerbated by small sample sizes (*e.g.*, n = 3) for a given CNT type and dose. The following independent variables are associated with each group of DBPs: DOC ratio, UV_{254} ratio, CNT dose, carbon–carbon bonds, alcohol groups, carbonyl groups, carboxyl groups, S_{BET}, and cumulative pore volume (CPV). A binary variable (called water type) distinguishing between water types was also included in models of TTHM and DHAN ratio. A binary variable was deemed more appropriate than including water quality characteristics as individual independent variables because these characteristics do not vary among the samples of a given water type. This variable was only used for TTHM and DHAN ratio because TONO ratio does not include samples of BL-RAW that were below the MDL. DOC and UV_{254} ratio were calculated using procedures analogous to DBP ratio and were incorporated into the numerical models to assess their usefulness as DBP precursor surrogates, as opposed to the other independent variables related to CNT properties. An additional binary variable distinguishing single- and multi-walled CNTs is explored in the ESI.† Analysis of variance was used to study associations between DBP ratios and independent variables, or explanatory factors; equivalent linear regression was used to test hypotheses about factor levels while controlling for other factors. Models were estimated using STATA/IC 11.2 statistical software[32] which leverage principles of applied regression analysis as detailed by Draper and Smith.[33]

3. Results and discussion

3.1. DBP precursor adsorption by CNTs

Fig. 1 shows percent removals of TTHMFP and DHANFP from BL-RAW (Fig. 1A) and of TTHMFP, DHANFP, and TONOFP from WS-EFF (Fig. 1B) attributed to each of the nine CNT types. Removal of TONOFP is only provided for WS-EFF because the concentration was below the MDL in BL-RAW. DBPFP removal is assumed to be due to adsorption of DBP precursors by the CNTs. As expected, increasing the CNT dose from 25 to 50 mg L^{-1} resulted in an increase in percent removal for each DBP precursor for all nine CNT types. For TTHM precursor removal, the CNT types assessed performed similarly or better on a percent basis than the activated carbons used by Najm and colleagues[34] and Iriarte-Velasco *et al.*[35] Additionally, Iriarte-Velasco and colleagues reported removal of DOC (a commonly used as a TTHM precursor surrogate) as 27.6 and 2.2 mg DOC g^{-1} GAC for two types of GAC tested. In comparison, the removal of DOC from BL-RAW ranged from 8.5–24.2 mg DOC g^{-1} CNT, while the removal from WS-EFF was 11.4–57.1 mg DOC g^{-1} CNT, depending on the CNT type. DHAN can be formed through two pathways

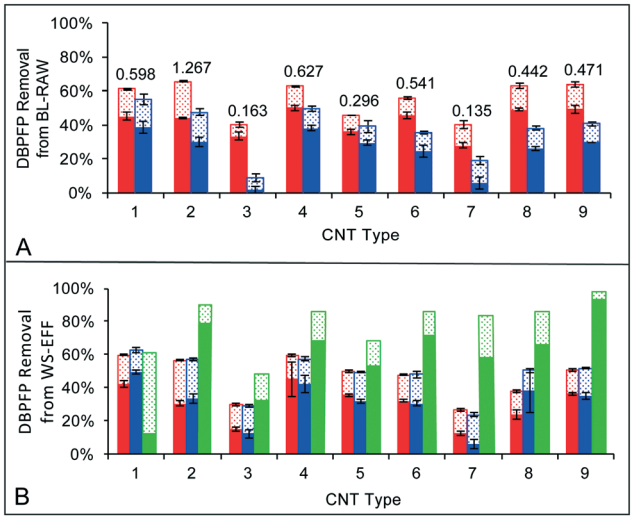

Fig. 1 Percent removal of TTHMFP (■ 25 mg L^{-1} CNT dose, □ 50 mg L^{-1} CNT dose), DHANFP (■ 25 mg L^{-1} CNT dose, □ 50 mg L^{-1} CNT dose) and TONOFP (■ 25 mg L^{-1} CNT dose, □ 50 mg L^{-1} CNT dose) by nine CNT types from Beaver Lake raw water (BL-RAW, Fig. 1A) and West Side wastewater treatment plant effluent (WS-EFF, Fig. 1B). Values above bars in Fig. 1A correspond to the CPV (cm^3 g^{-1}) of each CNT type and hold true in Fig. 1B as well. For TTHMFP and DHANFP, 95% confidence intervals are shown based on triplicate samples on a molar basis. Average FP for untreated BL-RAW samples was 0.095 and 0.022 μmol L^{-1} for TTHMs and DHANs respectively and 0.250 and 0.086 μmol L^{-1} respectively in WS-EFF. TONOFP was measured for WS-EFF only in mass-based units as NDMA with an average concentration of 400 ng L^{-1} as NDMA for untreated samples.

utilizing different reactants, which include: (1) the decarboxylation pathway, in which chloramine (and/or free chlorine) reacts with amine-containing moieties of NOM and (2) the aldehyde pathway, where an aldehyde incorporates chloramine–nitrogen.[36] For BL-RAW samples, the percent removals of DHAN precursors were less than that of TTHM precursors for all nine CNT types; in contrast, for WS-EFF samples, removal of DHAN precursors by CNT types 1, 2, and 8 surpassed removal of TTHM precursors. Though other precursors in natural waters may contribute to DHANFP in an unknown degree, this relative difference in precursor removal between BL-RAW and WS-EFF suggests the possibility either the amine- or aldehyde-based precursors are more prevalent in WS-EFF and have a greater affinity for CNTs than the less abundant precursors.

Average percent removal of TONO precursors reached a maximum of 93% (type 9) at a CNT dose of 25 mg L^{-1} and 97% at the higher CNT dose. Because of a lack of similar studies involving CNTs and TONO precursors, direct comparisons to the literature are not possible. However, using linear interpolation, we compared these results to Hanigan *et al.*[37] who quantified NDMA precursor adsorption in batch studies with activated carbon and found that 6 of the 9 CNT types achieved approximately the same or higher percent removals of TONO precursors on a mass sorbent basis. It is important to note that NDMA may only comprise ~5% of TONO formed

following chloramination of wastewater effluent organic matter[11] and little is known about the physicochemical properties of TONO precursors relative to NDMA precursors. Additionally, the average percent removal of TONO precursors at the 50 mg L^{-1} CNT dose was 31% greater than either TTHM or DHAN precursor removal. Hydrophilic base fractions of organic matter are considered the most likely *N*-nitrosamine precursors in DWTPs[38] and WWTP effluent.[39] Taken together, this may indicate that CNTs can sorb both hydrophobic and hydrophilic NOM fractions from natural waters although additional testing is required to support such an assertion. Regardless, the results in Fig. 1B illustrate that many CNT types have high affinities for TONO precursors, the underlying reasons for which are discussed further in section 3.3.

3.2. CNT characterization

The physical and chemical characteristics of each CNT type are summarized in Table 1. The shape of the gas adsorption isotherms (Fig. S1†) indicated the nitrogen adsorption isotherms were IUPAC type II and the carbon dioxide adsorption isotherms were type I.[40–42] CPV varied almost one order of magnitude, from 0.135 $cm^3\ g^{-1}$ (type 7) to 1.267 $cm^3\ g^{-1}$ (type 2). The CPV measurements of all CNT types fell within the range of values reported in the literature (0.104–2.46 $cm^3\ g^{-1}$), which vary based on CNT dimensions and the number of walls and are associated with both pristine and modified CNTs.[41–43] Pore volume distributions were bimodal (Fig. S2†), with microporosity assumed to be associated with the interstitial space within CNT bundles and mesoporosity associated with the space within individual tubes.[44] S_{BET} measurements (Table 1) were within 55% of supplier specifications (Table S2†) in all cases with the exception of type 2, which was 106% greater. In fact, S_{BET} for type 2 (837 $m^2\ g^{-1}$) was higher than the range reported in the literature for SWCNTs (22–662 $m^2\ g^{-1}$).[19,42] However, S_{BET} can vary based on CNT dimensions and the methods of synthesis and purification, and thus, values outside the ranges reported in the literature are not unexpected. For all MWCNT types, S_{BET} fell within the range reported in the literature (58–653 $m^2\ g^{-1}$).[19,21,42,43] Elemental composition data from deconvolution of carbon spectra from XPS measurements (Fig. S3†) indicated that surface oxides (*i.e.*, the sum of C–O, C═O, and COO functional groups) comprised 11% (type 7) to 14% (type 2) of the CNTs (Table 1), which falls into the range (6–32%) reported by others.[45,46] In section 3.3, we explore relationships between CNT properties and DBP precursor adsorption.

3.3. Impacts of physicochemical CNT properties on DBP precursor adsorption

Multivariate analysis for each DBP type yielded regression coefficients and *p*-values (Table 2) for TTHM (n = 36), DHAN (n = 36) and TONO (n = 18). Coefficients with $p < 0.05$ are assumed to be nonzero and indicate a significant effect on DBP ratio (*i.e.*, influent-normalized effluent concentration), controlling for other variables in the model. Significance of an independent variable in the negative direction indicates that an increase in the magnitude of that variable resulted in a decrease in DBP ratio, otherwise stated as an increase in the removal of that DBP precursor by the nine CNT types. A scatterplot of residuals *versus* fitted values suggested constant error variance (Fig. 2A–C). *R*-squared values indicated strong correlations between fitted values and observed values of DBP ratio for TTHM (R^2 = 0.92, Fig. 2D), DHAN (R^2 = 0.92, Fig. 2E) and TONO (R^2 = 0.96, Fig. 2F). In essence, the model has no discernible bias to the magnitude of DBP ratio and at least 92% of the variation is explained by the measured CNT properties.

The regression coefficients and *p*-values in Table 2 indicate several notable trends. Opposing signs of significance for the water type binary variable for TTHM ratio and DHAN ratio indicate that in comparing DBP precursor removal from the two waters, there was greater removal of (1) TTHM precursors from BL-RAW and (2) DHAN precursors from WS-EFF samples when controlling for all other variables in the model. Also, across all three DBP groups, an increase in either CNT dose or the amount of carboxyl groups resulted in greater removal of precursors. That CNT dose shows this trend only

Table 1 Physical and chemical characteristics of the selected CNTs

	Physical characteristics from SAA[a]		Relative amount of chemical bonds from XPS[b]			
CNT type	CPV[c] ($cm^3\ g^{-1}$)	S_{BET}[d] ($m^2\ g^{-1}$)	C═C or C–C[e]	C–O[f]	C═O[g]	COO[h]
1	0.598	446	77.75	8.56	2.70	1.83
2	1.267	837	73.83	10.25	2.90	1.09
3	0.163	104	78.55	7.07	2.98	1.45
4	0.627	426	75.09	8.53	3.90	2.23
5	0.296	171	76.89	7.86	2.65	2.11
6	0.541	298	78.17	7.72	2.88	1.73
7	0.135	92	80.85	6.76	1.81	1.97
8	0.442	265	78.40	7.80	2.18	1.98
9	0.471	262	77.13	7.45	3.00	1.91

[a] Quantachrome Nova 2200e surface area and pore size analyzer. [b] PHI 5000 VersaProbe X-ray photoelectron spectrometer, reported as the percent of total carbon bond types present and does not include shake-up features. [c] Cumulative pore volume. [d] Surface area calculated using the Brunauer–Emmett–Teller (BET) model. [e] Analyzed as total of C═C, C–C, and C–H bonds. [f] Alcohol bonds. [g] Carbonyl bonds. [h] Carboxyl bonds.

Table 2 Linear regression models of DBP ratio for TTHMFP, DHANFP and TONOFP

Independent variables[a]	TTHMFP ratio		DHANFP ratio		TONOFP ratio	
	Coeff.[b]	*p*-value	Coeff.	*p*-value	Coeff.	*p*-value
DOC ratio	0.618*	0.000	0.427*	0.005	1.667	0.097
UV_{254} ratio	0.039	0.731	0.384*	0.003	−1.900**	0.016
Water type[c]	−0.099**	0.000	0.050*	0.009	—	—
CNT dose (mg L^{-1})	−0.004**	0.000	−0.003**	0.006	−0.011**	0.001
Carbon–carbon bonds	0.018	0.441	0.002	0.918	−0.014	0.823
Alcohol groups (%)	0.028	0.682	−0.081	0.264	0.445*	0.016
Carbonyl groups (%)	−0.007	0.859	0.026	0.537	−0.089	0.462
Carboxyl groups (%)	−0.112**	0.002	−0.212**	0.000	−0.246**	0.010
BET surface area (m^2 g^{-1})	−0.000	0.837	0.001	0.239	0.000	0.798
CPV[d] (mL g^{-1})	−0.096	0.679	−0.376	0.140	−2.246**	0.001
Constant	−1.034	0.666	0.919	0.710	−0.042	0.994

*Positive significance ($p < 0.05$).**Negative significance ($p < 0.05$).[a] Independent variables all represent terms in regression equations. [b] Regression coefficients. [c] Binary variable distinguishing between BL-RAW and WS-EFF samples, not applicable to TONO ratio. [d] Cumulative pore volume.

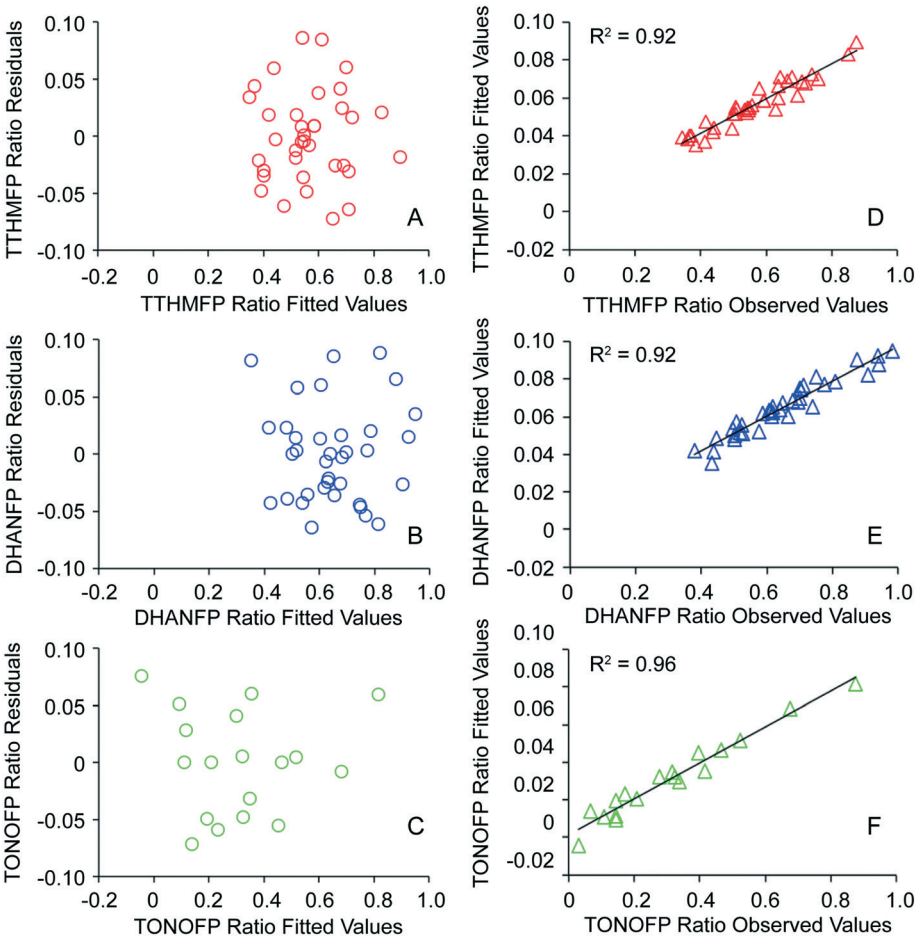

Fig. 2 Error variance of models for TTHMFP ratio (Fig. 2A), DHANFP ratio (Fig. 2B) and TONOFP (Fig. 2C) and representations of model correlations with observed values of TTHMFP, DHANFP and TONOFP ratios (Fig. 2D–F). Independent variables used to fit models of TTHMFP, DHANFP, and TONOFP ratio are detailed in Table 2.

confirms the effect of these particular dosages illustrated in Fig. 1. However, the relationship between DBP ratio and the percent of carboxyl groups is intriguing due to the significance of that variable across all DBP groups and suggests that CNT surface chemistry is important for DBP precursor adsorption. For TONO ratio only, a positive correlation with the percent of alcohol functional groups indicates a decrease in the amount of those surface oxides increased adsorption

of TONO precursors. Additionally, for TONO ratio alone, there was a significant relationship with CPV, indicating that an increase in CPV resulted in enhanced TONO precursor removal. Notably, true relationships between DBP precursor removal and CNT surface chemistry would be obscured by large errors in XPS carbon spectra deconvolution or any other independent variable. The risk of accidentally or randomly observing a relationship that is untrue is kept low by the choice of significance level (alpha = 0.05). Therefore, we have confidence in the importance of significant chemical characteristics in the models.

Surface oxides are generally considered to inhibit sorption of NOM (*i.e.*, DBP precursors) to activated carbon due to repulsion caused by their negative surface charge.[47] However, the results of the multivariate model (Table 2) indicate that an increase in carboxyl groups increases adsorption of all three groups of DBP precursors. Zhang *et al.*[48] postulated a link between chemical and physical CNT characteristics that may be relevant here: repulsive forces created by negatively charged oxygen-containing functional groups enlarge spaces between individual CNTs in bundles thereby increasing CPV and S_{BET}. Additionally, functional groups generally form at defect sites in the CNT walls which are also locations that allow access inner microporosity or mesoporosity (depending on the inner diameter of the CNT).[44] It has also been shown that the presence of surface oxides increases the hydrophilicity of CNT surfaces, which could enhance the adsorption of hydrophilic DBP precursors, such as those that react with chloramines to form *N*-nitrosamines.[48] Additionally, amine-based groups serving as *N*-nitrosamine precursors are positively charged at circumneutral pH. Thus, these groups would experience electrostatic attractions to the negatively charged carboxylic acid functionalities on the CNTs, which may explain the high removal of TONO precursors relative to TTHM and DHAN precursors. Hydrogen bonding may also be an important adsorption mechanism, which would be consistent with our results, as increases in oxygen groups will increase adsorption when hydrogen bonding is important.[49] However, application of CNTs in the water produces hydrophobic interactions that could obscure the contribution of hydrogen bonding as an adsorption mechanism. The multicollinearity of the physical and chemical properties indicates that both CPV and oxygen-containing functional groups are important to CNT performance for DBP precursor removal.

To explore the concept of DBP precursor size exclusion from the CNT pore networks, linear regression models were refit for all DBP types by arbitrarily increasing minimum pore widths used for the computation of pore volume while all other variables remained unchanged (Fig. 3). For TTHM, CPV *p*-values were large ($p > 0.5$) at low pore widths (<5 nm) and only came close to significance ($p = 0.079$) above 15 nm. For DHAN, CPV *p*-values decreased from ~0.15 and became significant ($p = 0.05$) near a minimum pore width of 7 nm and remained significant throughout. For TONOFP, pore volume had a negative effect (*i.e.* more precursor adsorption occurred as pore volume increased) and pore width had relatively little

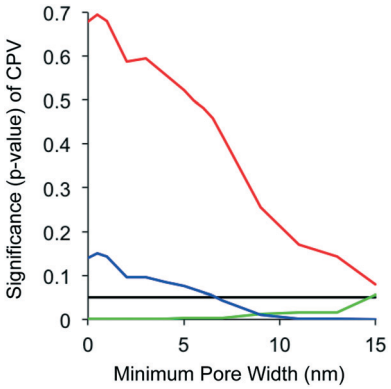

Fig. 3 Significance of cumulative pore volume (CPV) in linear regression models (see Table 2) of TTHMFP ratio (—), DHANFP ratio (—) and TONOFP ratio (—) as calculated by arbitrarily increasing the minimum pore widths used to calculate CPV for all nine types of carbon nanotubes. A *p*-value of 0.05 is included to illustrate the point below which CPV is statistically significant.

impact on the importance of pore volume. On balance, the results in Fig. 3 indicate that size exclusion effects by the CNT pores could impact adsorption of TTHM and DHAN precursors, but not TONO precursors. The trends in Fig. 3 could indicate that TONO precursors are generally smaller in size (or more accessible to the smaller CNT pores) than TTHM and DHAN precursors. At smaller pore widths, TONO precursors may not have much competition for adsorption sites; as pore width increases toward pores in excess of 15 nm, larger and more abundant TTHM and DHAN precursors could utilize a greater portion of the adsorption capacity. Others have shown that larger molecules at relatively high concentrations (such as TTHM precursors) can block CNT pores and limit further adsorption, while small molecules at trace concentrations (such as TONO precursors) experience little competition for adsorption sites.[50]

3.4. Fluorescence metrics as DBP precursor surrogates

Fluorescence EEMs were measured on untreated and CNT-treated (but not chloraminated) waters to evaluate its usefulness as a precursor surrogate and perhaps limit time-consuming DBPFP analyses in upcoming studies. Fluorescence intensities at all wavelength pairs measured were regressed against the DBP data to identify pairs for which strong correlations exist. Fig. 4 shows the correlation coefficients presented on axes equivalent to the EEMs for TTHMFP (panel A, $R_{MAX}^2 = 0.86$), DHANFP (panel B, $R_{MAX}^2 = 0.88$), and TONOFP (panel C, $R_{MAX}^2 = 0.50$) in WS-EFF, and TTHMFP (panel D, $R_{MAX}^2 = 0.78$) and DHANFP (panel E, $R_{MAX}^2 = 0.80$) in BL-RAW. These correlations represent relationships between DBP precursors remaining after treatment with CNTs and DBP concentrations formed following FP tests, performed using a recently developed method.[16] As expected, correlations are strong for TTHMFP and DHANFP in both waters. However, the moderate correlation coefficients for

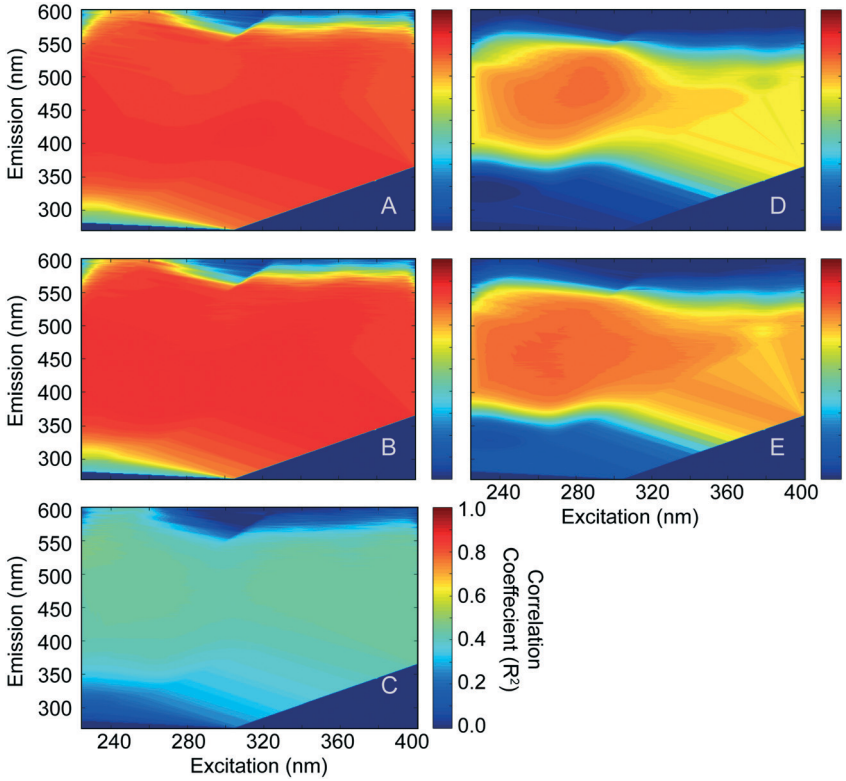

Fig. 4 Correlation coefficients for fluorescence intensities of WS-EFF samples in relation to TTHMFP (Fig. 4A), DHANFP (Fig. 4B) and TONOFP (Fig. 4C) and of BL-RAW samples in relation to TTHMFP (Fig. 4D) and DHANFP (Fig. 4E).

TONOFP indicate that fluorescence is unlikely to be a suitable precursor surrogate for total *N*-nitrosamine precursor concentrations when applied in this manner. Interestingly, samples from WS-EFF (Fig. 4A and B) show a large region of wavelength pairs that give high correlation coefficients. In contrast, high R_{MAX}^2 values for BL-RAW (Fig. 4D and E) are more localized and are centered near $I_{275/480}$. The insensitivity in R^2 values shown in Fig. 4A–C was unexpected in light of several studies attributing the various regions of EEMs to distinct fluorophore groups (*i.e.*, humic-, fulvic-, tryptophan-, and tyrosine-like), each with its unique chemistry.[51] The results presented in Fig. 4 suggest strong relationships among virtually all wavelength pairs, and thus imply interdependence (*i.e.* an increase in a particular fluorophore group could impact other regions of the EEM). Fluorescence EEMs were also analyzed by PARAFAC analysis. A detailed discussion of the removal of the PARAFAC components by the CNTs and correlations between PARAFAC components (Table S5†) is provided in the ESI.† This analysis advances our assertion of fluorophore interdependence, which prevents valid conclusions regarding the affinity of CNTs for discrete humic-, fulvic- and protein-like fluorophores. The interdependence observed in both EEM correlations and PARAFAC components may be indicative of interferences on the protein-like fluorophores and preclude the use of fluorescence EEMs alone as a surrogate for TONO precursors. However, the nature of these precursors suggests that fluorescence may be utilized following elimination of interfering humics,[52] in applications such as asymmetric flow field-flow fractionation where proteins can be physically separated from humics prior to fluorescence measurements.

3.5. Implications

Based on the importance of surface oxides and CPV for DBP precursor removal, future studies are needed to enhance these CNT characteristics and test their impact in sorption systems. Oxidative treatment with a mixture of nitric and sulfuric acid has been shown to result in formation of oxygen-containing groups on SWCNTs[18,46] and MWCNTs.[45] Additionally, KOH treatment can increase surface area and pore volume, specifically in mesopores.[53] Based on the size exclusion results (Fig. 3), this may be particularly important to improve sorption of DHAN and TTHM precursors. Furthermore, future studies of CNT modification should be paired with a reliable system for CNT integration into DWTP treatment processes. A large range of possibilities now exists regarding design of freeform CNT microstructures grown on substrates that could be adapted into current treatment processes. These microstructures can be grown to exacting specifications of size, shape, and porosity, and conformal coating can be applied to manipulate chemical properties.[1] Additionally, incorporation of CNTs into hollow fiber membranes has been shown to increase membrane flux, fouling resistance, thermal stability, porosity, and electrochemically regenerative capability with minimal CNT leaching.[54–56]

4. Conclusions

With no modification, CNTs have natural affinity for THM-, DHAN, and TONO precursors. The breadth of applications discovered for CNTs due to their unique set of physiochemical properties speak to their potential for further commercial availability. Though CNTs are a novel sorbent with higher costs than standard sorbents, higher performance levels – particularly with regard to TONO precursor adsorption – give CNTs an advantage that warrants future study. As production costs decrease and the body of research regarding their applications increases, CNTs gain potential for feasibility of application in conventional water treatment systems. Manipulation of physicochemical properties to enhance DBP precursor adsorption in concert with reliable methods of integration into water treatment processes could provide DWTPs with a new technique for meeting the increasingly rigorous water quality standards for DBP control.

Acknowledgements

Financial support from the National Science Foundation (CBET #1254350 to JLF) and the University of Arkansas Doctoral Academy Fellowship (to EMN) is gratefully acknowledged. The authors thank Thien Do and Huong Pham (PhD students, University of Arkansas) and two anonymous reviewers for their constructive comments on previous versions of this manuscript.

References

1 M. De Volder, S. Park, S. Tawfick and A. J. Hart, *Nat. Commun.*, 2014, **5**, 4512.
2 S. Tawfick, M. De Volder, D. Copic, S. J. Park, C. R. Oliver, E. S. Polsen, M. J. Roberts and A. J. Hart, *Adv. Mater.*, 2012, **24**, 1628–1674.
3 R. Das, S. B. A. Hamid, M. E. Ali, A. F. Ismail, M. S. M. Annuar and S. Ramakrishna, *Desalination*, 2014, **354**, 160–179.
4 Y. Liu, Y. Zhao, B. Sun and C. Chen, *Acc. Chem. Res.*, 2013, **46**, 702–713.
5 K. Yang and B. Xing, *Environ. Pollut.*, 2009, **157**, 1095–1100.
6 J. J. Rook, *J. - Am. Water Works Assoc.*, 1976, **68**, 168–172.
7 S. W. Krasner, H. S. Weinberg, S. D. Richardson, S. J. Pastor, R. Chinn, M. J. Sclimenti, G. D. Onstad and A. D. Thruston, *Environ. Sci. Technol.*, 2006, **40**, 7175–7185.
8 S. W. Krasner, W. A. Mitch, D. L. McCurry, D. Hanigan and P. Westerhoff, *Water Res.*, 2013, **47**, 4433–4450.
9 *Disinfection by-products and human health*, ed. S. E. Hrudey and J. W. A. Charrois, IWA Publishing and Australian Water Association, London, 2012.
10 C. G. Russell, N. K. Blute, S. Via, X. Wu and Z. Chowdhury, *J. - Am. Water Works Assoc.*, 2012, **104**, E205–E217.
11 N. Dai and W. A. Mitch, *Environ. Sci. Technol.*, 2013, **47**, 3648–3656.
12 N. Dai, A. D. Shah, L. H. Hu, M. J. Plewa, B. McKague and W. A. Mitch, *Environ. Sci. Technol.*, 2012, **46**, 9793–9801.
13 X. Wang, S. Tao and B. Xing, *Environ. Sci. Technol.*, 2009, **43**, 6214–6219.
14 A. D. Pifer and J. L. Fairey, *Environ. Eng. Sci.*, 2014, **31**, 117–126.
15 C. A. Stedmon and R. Bro, *Limnol. Oceanogr.: Methods*, 2008, **6**, 572–579.
16 T. D. Do, J. R. Chimka and J. L. Fairey, *Environ. Sci. Technol.*, 2015, **49**, 9858–9865.
17 X. B. Liao, C. K. Wang, J. Wang, X. J. Zhang, C. Chen, S. W. Krasner and I. H. Suffet, *J. - Am. Water Works Assoc.*, 2014, **106**, 81–82.
18 K. Balasubramanian and M. Burghard, *Small*, 2005, **1**, 180–192.
19 M. E. Birch, T. A. Ruda-Eberenz, M. Chai, R. Andrews and R. L. Hatfield, *Ann. Occup. Hyg.*, 2013, **57**, 1148–1166.
20 Y.-H. Shih and M.-S. Li, *J. Hazard. Mater.*, 2008, **154**, 21–28.
21 H.-H. Cho, B. A. Smith, J. D. Wnuk, D. H. Fairbrother and W. P. Ball, *Environ. Sci. Technol.*, 2008, **42**, 2899–2905.
22 X. Ren, C. Chen, M. Nagatsu and X. Wang, *Chem. Eng. J.*, 2011, **170**, 395–410.
23 V. K. K. Upadhyayula, S. Deng, M. C. Mitchell and G. B. Smith, *Sci. Total Environ.*, 2009, **408**, 1–13.
24 S. Sen, B. E. Haggard, I. Chaubey, K. R. Brye, T. A. Costello and M. D. Matlock, *Water, Air, Soil Pollut.*, 2007, **179**, 67–77.
25 In *Standard Methods for the Examination of Water & Wastewater*, ed. A. D. Eaton, L. S. Clesceri, E. W. Rice and A. E. Greenberg, American Public Health Association, Washington, DC, 2005.
26 C. Y. Lu and F. S. Su, *Sep. Purif. Technol.*, 2007, **58**, 113–121.
27 T. Karanfil, I. Erdogan and M. A. Schlautman, *J. - Am. Water Works Assoc.*, 2003, **95**, 86–100.
28 A. D. Pifer and J. L. Fairey, *Water Res.*, 2012, **46**, 2927–2936.
29 P. Kulshrestha, K. C. McKinstry, B. O. Fernandez, M. Feelisch and W. A. Mitch, *Environ. Sci. Technol.*, 2010, **44**, 3369–3375.
30 W. A. Mitch and N. Dai, *Development and application of a total nitrosamine assay for disinfected waters*, Water Research Foundation, Web Report #4209, 2012.
31 Y. W. Zhu, S. Murali, M. D. Stoller, K. J. Ganesh, W. W. Cai, P. J. Ferreira, A. Pirkle, R. M. Wallace, K. A. Cychosz, M. Thommes, D. Su, E. A. Stach and R. S. Ruoff, *Science*, 2011, **332**, 1537–1541.
32 StataCorp (2009). *Stata Statistical Software: Release 11*, College Station, TX, StataCorp LP.
33 N. R. Draper and H. Smith, *Applied regression analysis*, John Wiley & Sons, Inc., New York, 1998.
34 I. N. Najm, V. L. Snoeyink, B. W. Lykins and J. Q. Adams, *J. - Am. Water Works Assoc.*, 1991, **83**, 65–76.
35 U. Iriarte-Velasco, J. I. Alvarez-Uriarte, N. Chimeno-Alanis and J. R. Gonzalez-Velasco, *Ind. Eng. Chem. Res.*, 2008, **47**, 7868–7876.
36 A. D. Shah and W. A. Mitch, *Environ. Sci. Technol.*, 2012, **46**, 119–131.
37 D. Hanigan, J. Zhang, P. Herckes, S. W. Krasner, C. Chen and P. Westerhoff, *Environ. Sci. Technol.*, 2012, **46**, 12630–12639.
38 C. K. Wang, X. J. Zhang, J. Wang, S. M. Liu, C. Chen and Y. F. Xie, *Sci. Total Environ.*, 2013, **449**, 295–301.
39 E. Pehlivanoglu-Mantas and D. L. Sedlak, *Water Res.*, 2008, **42**, 3890–3898.

40 K. S. W. Sing, D. H. Everett, R. A. W. Haul, L. Moscou, R. A. Pierotti, J. Rouquerol and T. Siemieniewska, *Pure Appl. Chem.*, 1985, **57**, 603–619.
41 B. Adeniran and R. Mokaya, *J. Mater. Chem. A*, 2015, **3**, 5148–5161.
42 S. Zhang, T. Shao, H. S. Kose and T. Karanfil, *Environ. Sci. Technol.*, 2010, **44**, 6377–6383.
43 O. G. Apul and T. Karanfil, *Water Res.*, 2015, **68**, 34–55.
44 C. M. Yang, D. Y. Kim and Y. H. Lee, *J. Nanosci. Nanotechnol.*, 2005, **5**, 970–974.
45 H. Ago, T. Kugler, F. Cacialli, W. R. Salaneck, M. S. P. Shaffer, A. H. Windle and R. H. Friend, *J. Phys. Chem. B*, 1999, **103**, 8116–8121.
46 N. Y. S. Komarova, A. G. Krivenko, A. G. Ryabenko, A. V. Naumkin, K. I. Maslakov and S. V. Savilov, *J. Electroanal. Chem.*, 2015, **738**, 27–34.
47 T. Karanfil, W. Cheng, S. Dastgheib, Y. Guo and H. Song, *DBP formation control by modified activated carbons*, Awwa Research Foundation, Denver, CO, 2007.
48 Y. Zhang, C. Chen, L. Peng, Z. Ma, Y. Zhang, H. Xia, A. Yang, L. Wang, D. S. Su and J. Zhang, *Nano Res.*, 2015, **8**, 502–511.
49 B. Pan and B. Xing, *Environ. Sci. Technol.*, 2008, **42**, 9005–9013.
50 D. Hanigan, J. Zhang, P. Herckes, E. Zhu, S. Krasner and P. Westerhoff, *J. - Am. Water Works Assoc.*, 2015, **107**, 90–91.
51 N. Hudson, A. Baker and D. Reynolds, *River Res. Appl.*, 2007, **23**, 631–649.
52 Z. G. Wang, J. Cao and F. G. Meng, *Water Res.*, 2015, **68**, 404–413.
53 J. J. Niu, J. N. Wang, Y. Jiang, L. F. Su and J. Ma, *Microporous Mesoporous Mater.*, 2007, **100**, 1–5.
54 H. Huang, H. Fairbrother, B. Teychene, G. Ajmani, T. A. Chalew, M. J. Gallagher, H. Cho, K. Schwab and J. Jacangelo, *Water Sci. Technol.: Water Supply*, 2014, **14**, 917–923.
55 A. Jafari, A. H. Mahvi, S. Nasseri, A. Rashidi, R. Nabizadeh and R. Rezaee, *J. Environ. Health Sci. Eng.*, 2015, **13**, 51.
56 G. Wei, H. Yu, X. Quan, S. Chen, H. Zhao and X. Fan, *Environ. Sci. Technol.*, 2014, **48**, 8062–8068.